Journal of Materials Science and Chemical Engineering, 2015, 3, 29-36
Published Online January 2015 in SciRes. http://www.scirp.org/journal/msce
http://dx.doi.org/10.4236/msce.2015.31005

Synthesis of Nanostructured TiO_2 Photocatalyst with Ultrasonication at Low Temperature

Yong Tao[1], Zhenan Han[1], Zuolian Cheng[2*], Qishan Liu[3], Fengxia Wei[1], Kok Eng Ting[2], Xi Jiang Yin[1]

[1]Advanced Materials Technology Center, Singapore Polytechnic, Singapore City, Singapore
[2]School of Chemical & Life Sciences, Singapore Polytechnic, Singapore City, Singapore
[3]School of Architecture & the Building Environment, Singapore Polytechnic, Singapore City, Singapore
Email: [*] cheng@sp.edu.sg

Received December 2014

Abstract

A thin film TiO_2 in hierarchical nano-structure with high photocatalytic activities was synthesized in simple steps with ultrasonication. The crystal structure and morphology of the photocatalyst were investigated by X-ray diffraction (XRD) and high-resolution field emission scanning electron microscope (FE-SEM). In the present work, nanostructured TiO_2 was directly formed onto a Ti substrate via a solution approach. This nanostructured TiO_2 photocatalyst can be reused and will not generate secondary contamination to treated water. The photocatalytic activity of the synthesized TiO_2 photocatalyst was evaluated by the degradation of phenol under UVC irradiation in water and was compared with the general sol-gel derived TiO_2 films as well as a commercial DP-25 TiO_2 coating. It was found that the synthesized nanostructured TiO_2has significantly high and stable photocatalytic activity.

Keywords

Photocatalysis, Ultrasonication, Semiconductor, Titanium Dioxide, Nanostructure

1. Introduction

Titanium dioxide (TiO_2) is one of the mostly studied semiconductors for various applications such as photocatalysts [1] [2], photovoltaic cells [3] [4], gas sensors [5], photonic crystals [6] and biomaterials [7]. Recently, semiconductors in nanostructure have drawn great interest [8] [9]. Some studies have appeared on preparation of TiO_2 nanotubes, nanowires, and especially, nanorods [10]-[12]. For example, Sugimoto *et al*. prepared TiO_2 (anatase) nanoparticles with shapes varying from round-cornered cubes to sharp-edged cubes by introducing amines as shape controllers in their so-called gel-sol method [10]. Yang *et al*. precipitated rod-like rutile from a $TiCl_4$/HCl solution exposed to a strong ultrasonic irradiation [11]. Pradhan *et al*. grew anatasenanorods on a

[*]Corresponding author.

How to cite this paper: Tao, Y., Han, Z.N., Cheng, Z.L., Liu, Q.S., Wei, F.X., Ting, K.E. and Yin, X.J. (2015) Synthesis of Nanostructured TiO_2 Photocatalyst with Ultrasonication at Low Temperature. *Journal of Materials Science and Chemical Engineering*, **3**, 29-36. http://dx.doi.org/10.4236/msce.2015.31005

WC-Co substrate at 873 K by metalorganic chemical vapor deposition (MOCVD) [12]. Nevertheless, these methods, together with the widely used approaches to obtain crystalline TiO_2 [13] [14], have particular drawbacks. TiO_2 prepared through hydrolysis and condensation of titanium alkoxides requires subsequent high-temperature thermal treatment (calcination e.g.) to induce crystallization and to remove the residual alkoxide groups [13] [14]. The high-temperature thermal process results in particle agglomeration, grain growth and therefore the reduced specific surface area. Although hydrothermal process, instead of the calcination, has been successfully used to induce crystallization, it requires high pressure and high temperature (usually > 413 K) conditions [10]. Well-crystallized TiO_2 can be obtained under mild conditions between ambient temperature to 373 K through the hydrolysis of the titanium (IV) inorganic salts of $TiCl_4$ [12] [15] [16], TiF_4 [17] and $TiOSO_4$ [18] [19] in aqueous phase; however, the counter anions of the starting titanium salts would remain in the products and deteriorate the purity of TiO_2 [17] [19]. In addition, $TiCl_4$ is so active that it should be used in a protective atmosphere at low temperature; whileTiF_4 is very expensive. Although MOCVD is an advanced technique, it requires stringent conditions to obtain crystalline TiO_2 nanorods [12].

Hydrogen peroxide (H_2O_2) is an oxidant bringing no secondary contaminations to the reaction system. In an attempt to verify the biocompatibility of titanium, Tengvall *et al*. studied the titanium peroxide gels derived through interactions between metallic Ti and H_2O_2 [20]. Ayers and Hunt prepared TiO_2 aerogels through the reaction of H_2O_2 with excess Ti followed by the subsequent solvent exchanges with ethanol and carbon dioxide, and supercritical drying [13]. Thermal treatment under argon at 473 K caused rapid decomposition of the aerogel, forming a blue-gray powder consisting of a mixture of rutile and anatase [13]. Wang *et al*. obtained anatase layer on Ti surface by heating (between 573 and 873 K) the amorphous TiO_2 gel formed through oxidizing Ti with 30 wt% H_2O_2 solution containing 3 mM $TaCl_5$ at 353 K for 1 h [21]. The present authors found that simply ageing this amorphous TiO_2 gel in water at 353 K can also induce crystallization which is in line with Wu *et al*. study [22]. This paper reported the preparation of well-crystallized nano TiO_2 with satisfying homogeneity through direct oxidation of metallic Ti with H_2O_2 at a low temperature of 353 K. To the authors' knowledge, this is the lowest temperature reported to prepare crystalline TiO_2 nanoflakes.

2. Experimental

2.1. Sample Preparation and Characterization

Ti plates (99.9% in purity, Titan Engineering, Singapore) with sizes of 12.5 × 15 × 1 cm^3 were pickled in the mixture of HF, HNO_3 and H_2O by volume ration of 1:3:6 at ambient temperature. After ultrasonically cleaning in deionized water, each piece of the Ti plate was soaked in a 50 ml H_2O_2 solution with different concentrations. The reactants were kept at 353 K with ultrasonication for a certain time in water bath. Then, the Ti plate was taken out and gently rinsed with deionized water and dried in oven. Ultrasonication and drying time, as well as concentration of H_2O_2 were tested systematically to study their influence on the photoctalysts activity. The morphology of as-prepared photocatalyst was observed via field emission scanning electron microscopy (FE-SEM, JEOL 6340F, Japan). Samples were characterized on X-ray diffraction (XRD, Bruker, Germany) with Cu Kα1 radiation (λ = 1.5406 Å). Surface elemental analysis was conducted on energy-dispersive X-ray detector equipped on the FESEM.

2.2. Evaluation of Photocatalytic Activity

The photocatalytic activity of the prepared Ti plates was conducted in a glass reactor in a blackbox at room temperature. The light source was a 9 W UVC spot light source. A piece of prepared TiO_2 plate (4.5 × 5 cm^2) was immersed into 100 mL of phenol solution (100 mg/L) for certain time. The reaction solution was magnetically stirred continuously during the photocatalytic reaction. Temperature variation throughout the reaction is less than 3 K. Phenol concentration change was analyzed by a high performance liquid phase chromatography (HPLC, LC-20AD, Shimadzu, Japan) with UV detector at a wavelength of 272 nm, using a 250 mm C15 RP column with particle size at 5 μm. The mobile phase employed was methanol/water (60/40) with flow rate at1 mL/min. Parallel experiments were carried out to ensure the reproducibility. The adsorption of phenol on the TiO_2 plate was assessed by the dark condition reaction. The photocatalytic activity of the Ti plate was defined as follows:

$$\mathrm{PA} = \left(1 - C_t / C_0\right) \times 100\% \quad (1)$$

where C_0 is the phenol initial concentration and C_t is the concentration at reaction time (t).

3. Results and Discussion

3.1. Morphology and Surface Structure

The morphology of the aged Ti plate is shown in **Figure 1**. Uniform photocatalyst thin layers were generated via H_2O_2 oxidization on both sides of the Ti plates (**Figure 1(a)**). **Figure 1(b)** shows densely packed microfibers with uniformly distributed nanoflakes which look like sea corals. High magnification FESEM images in **Figure 1(c)** and **Figure 1(d)** show the surface layer consisted of well-aligned nanoflakes with tens of nm in width and hundreds of nm in length. The XRD pattern in **Figure 3** shows that this surface layer is composed of well-crystallized anatase phase TiO_2.

As shown in **Figure 1(d)** of the cross-sectional FESEM image, the grown thin film has a depth of ca. 0.2 - 0.3 μm. The porosity and surface-to-volume ratios of the sample were greatly enhanced by these primary nanostructures, which could induce efficient diffusion and increased mass transfer of organic pollutant molecules within the microfibers architecture. The EDX spectra shows that the TiO_2 nanoflakes were elementally composed of only pure Ti and O with no extraneous elements from intermediates observed in the final anatase product.

Figure 2 shows the FESEM images of the samples prepared with and without ultrasonication. The nanostructure and density of the thin film prepared in water bath with ultrasonication is obviously finer than that obtained without ultrasonication. It could be attributed to the higher heating uniformity, lower temperature variation and higher heat transfer speed introduced by ultrasonication.

The as-prepared Ti plates were either dried in air or aged in oven at 80˚C for 8 h, respectively. The XRD patterns of the completed products in **Figure 3** shows that substantial crystallization of TiO_2 in an atasephase took place in the aging process, indicating that aging is not only helpful for surface stabilization, but also for the atomic diffusion and crystallization.

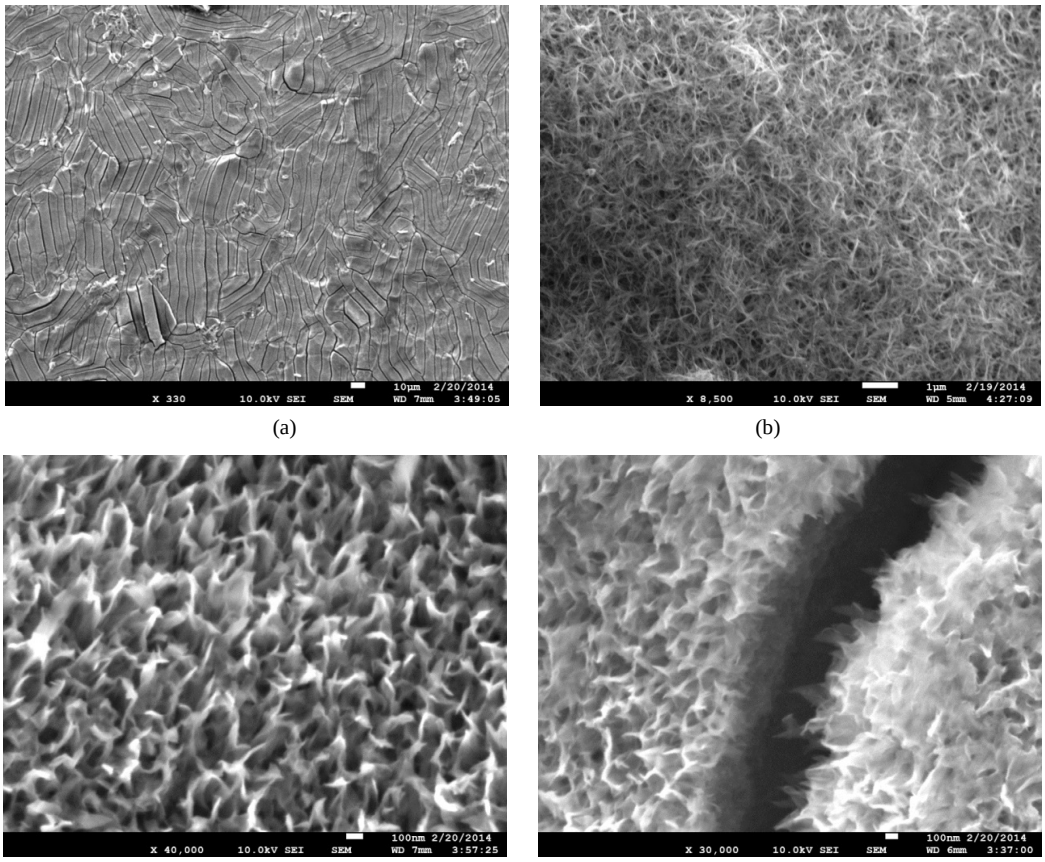

(a) (b)

(c) (d)

Figure 1. FESEM images of the aged Ti plate with different magnifications (80˚C for 8 h).

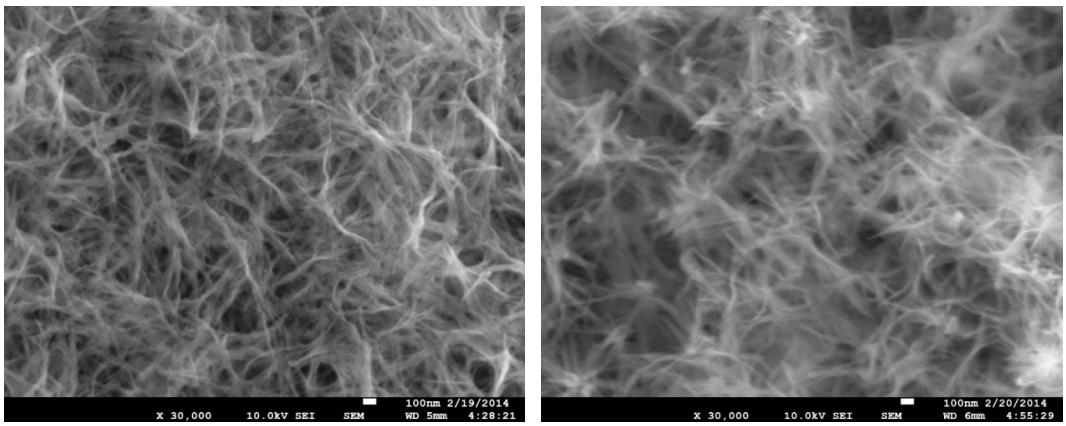

(a) (b)

Figure 2. FESEM morphology of the Ti plate surface prepared by soaking in 35 wt% H_2O_2 solution at 353 K for 72 h (a) with ultrasonication; (b) without ultrasonication.

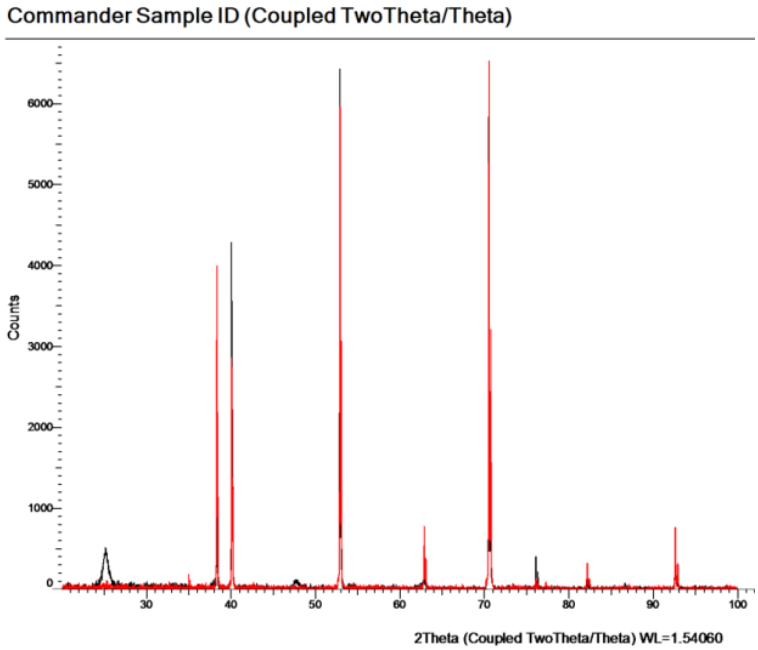

Figure 3. XRD patterns of the obtained TiO_2 nanoflakes. (a) Dried in air; (b) Aged at 80˚C for 8 h.

Figure 3(b) shows the XRD pattern of the TiO_2 nanoflakes harvested after aging. The obtained diffraction peaks are well matched with the JCPDS Card No.: 21-1272 indicating the body-centered tetragonal anatase phase TiO_2. The diffraction peaks at 2θ = 25.25˚ (101), 47.98˚ (200), 53.59˚ (106), 37.82˚ (004) and 62.36˚ (215) are all corresponding to the lattice plane of pureanatase phase. The absence of peaks at 2θ = 27.5˚ (110) and 30.8˚ (121) corresponding to rutile and brookite phase confirms the synthesized TiO_2 was in pure anatasephase [23]. The aged TiO_2 shows a wide (101) peak with more background disturbance indicating that the amorphous nature of the synthesized nanomaterials. However, no obvious peak was obtained for TiO_2 prepared without ultrasonication. The crystallite sizes are calculated from the broadening of the anatase (101) peaks using Scherer's formula.

$$D = K\lambda/(\beta\cos\theta) \quad (2)$$

where D is the crystallite size (nm), K is the shape constant (0.9), k is the wave length of Cu Kα1 radiation (1.5406 Å), θ is the diffraction angle (˚) and β is the full width at half maximum peak height. The crystallite size

of the air dried and aged TiO_2 is calculated as 14.8 and 4.65 nm, respectively. The result confirms that aging process helps crystallization of synthesized TiO_2 nanoflakes.

From the above investigation, it is clear that low-temperature aging of samples promoted the crystallinity of anatase formed and enhanced polymorph stability. Based on these results, the effect of H_2O_2 concentration was further studied. The oxidization reactions were conducted at 80˚C using four different concentrations (5%, 10%, 20% and 35%) of H_2O_2. **Figure 4** illustrates the SEM images of the surface morphology of the four samples. The uniformity and density of the grown nanoflakes are increased with increasing H_2O_2 concentration. **Figure 4(d)** demonstrates the largest density and contents of TiO_2 was obtained by 35 wt% H_2O_2.

3.2. Photocatalytic Degradation of Phenol

In order to evaluate the photocatalytic activity of the prepared photocatalyst, photocatalytic oxidation of phenol was carried out using catalysts prepared with different conditions as shown in **Figure 5**. Dark condition experiment with photocatalyst was carried out to examine the adsorption of phenol molecules on the catalyst surface. The control experiment was carried out with nophotocatalyst but with light only to evaluate the photolysis of phenol. Three replicates of all experiments were performed at identical conditions to perform error analysis.

Figure 5 shows that only a modest removal of phenol occurred in the control experiment (<20%) due to direct photolysis. While under dark condition with the synthesized photocatalyst, it is clear that limited amount of phenol was removed by adsorption. Comparing between samples prepared with/without ultrasonication, after 6 hours reaction, 94% and 72% of phenol was removed, respectively, which is in line with the surface morphology analysis.

Figure 6 shows the result of photocatalytic degradation of phenol with the air-dried and aged photocatalysts. The aged photocatalyst shows much better photocatalytic activity than that of the air-dried photocatalyst. The result can be attributed to the difference in UV light utilization by these two synthesized photocatalysts. Similar

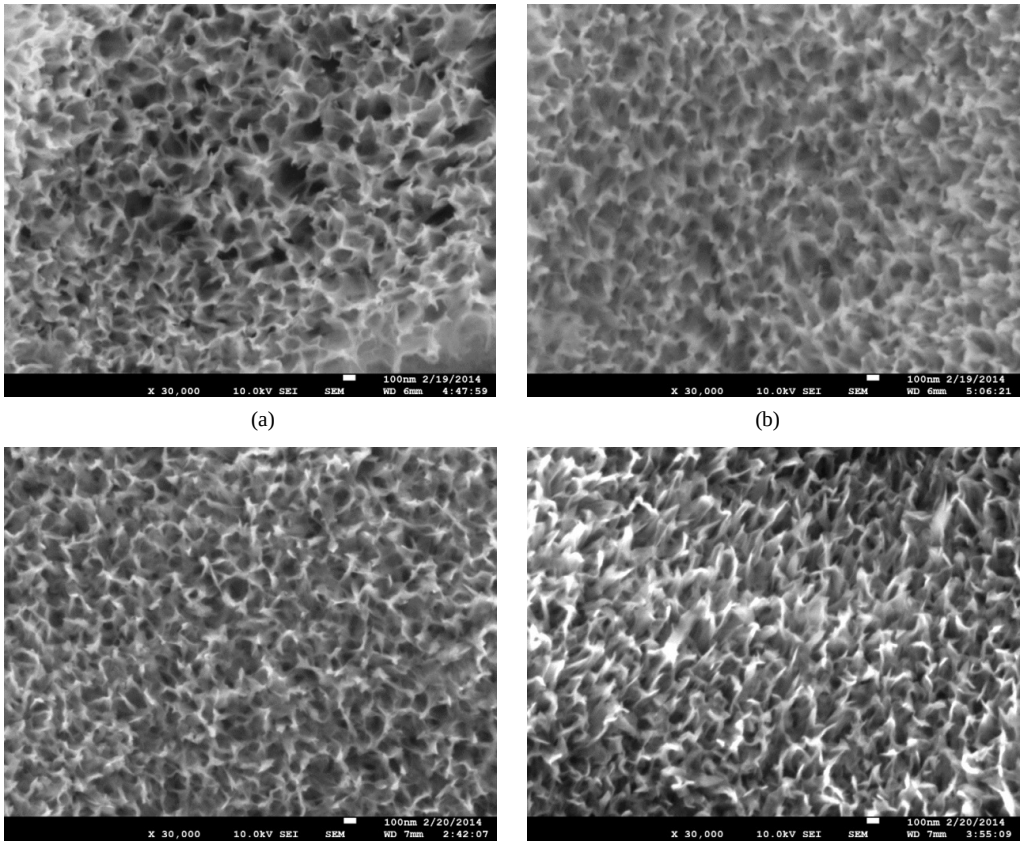

(a) (b)

(c) (d)

Figure 4. FESEM images of prepared samples: (a) 5% H_2O_2; (b) 10% H_2O_2; (c) 20% H_2O_2; (d) 35% H_2O_2.

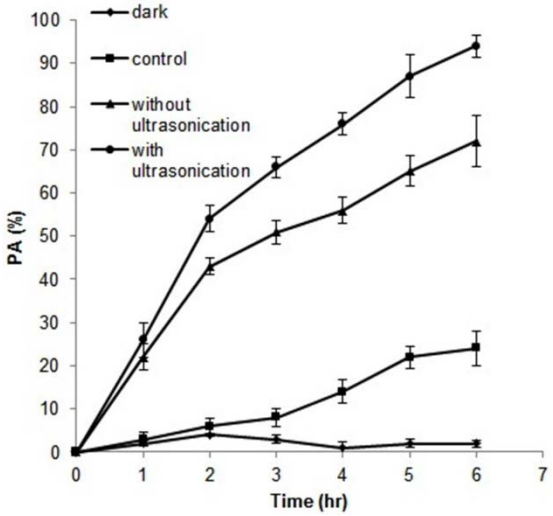

Figure 5. Effect from ultrasonication on the photocatalytic activity (PA) of the synthesized catalyst.

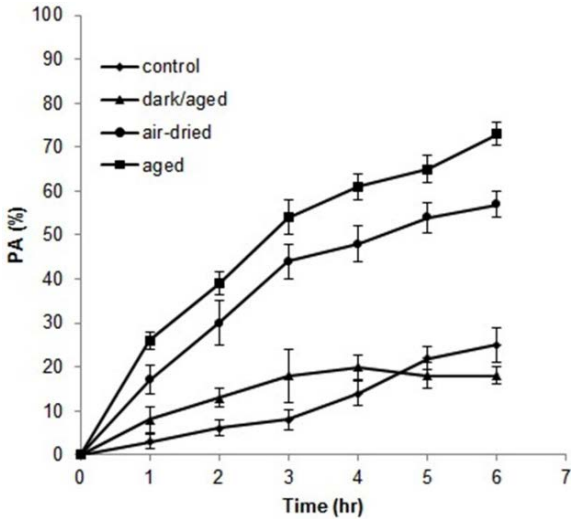

Figure 6. Effect from aging process on the photocatalytic activity (PA) of the synthesized catalyst.

results have been reported by other researchers on TiO_2 photocatalysts [24]. In general, photocatalytic activity depends on the efficiency of utilization of the incident radiation absorbed by the catalyst [25]. Due to amorphous nature of the air-dried TiO_2 photocatalyst, the scattering of incident UV light energy was more than the absorbed energy (results in decreased formation of electron and hole pairs) as compared to that of the aged catalyst, which may be resulted in decreased photocatalytic activity.

4. Conclusion

In summary, a one-step method involving an *in situ* oxidation process to synthesize highly crystallized, anatase TiO_2 photocatalysts with excellent photocatalytic activity has been developed. From practical point of view, the simple-to-operate strategy is favored by large scale production. The prepared nanostructured TiO_2 photocatalyst can be easily reused and will not generate secondary contamination to treated water. Fabrication conditions such as ultrosonication and post-synthesis aging can effectively improve the surface catalyst crystallization as well as the nanostructure formation, so that improving photocatalytic activity. Based on the catalytic performance of the synthesized nano-TiO_2, it is feasible to be commercialized as a fixed-bed reactor for industrial application.

Acknowledgements

This work is supported by Transfer Innovation Foundation of Singapore Ministry of Education (Grand No. MOE2012-TIF-2-G-034).

References

[1] Asahi, R., Morikawa, T., Ohwaki, T., Aoki, K. and Taga, Y. (2001) Visible-Light Photocatalysis in Nitrogen-Doped Titanium Oxides. *Science*, **293**, 269-271. http://dx.doi.org/10.1126/science.1061051

[2] Khan, S.U., Al-Shahry, M. and Ingler, W.B. (2002) Efficient Photochemical Water Splitting by a Chemically Modified n-TiO_2. *Science*, **297**, 2243-2245. http://dx.doi.org/10.1126/science.1075035

[3] Kraeutler, B. and Bard, A.J. (1977) Photoelectrosynthesis of Ethane from Acetate Ion at an n-Type Titanium Dioxide Electrode. The Photo-Kolbe Reaction. *Journal of the American Chemical Society*, **99**, 7729-7731. http://dx.doi.org/10.1021/ja00465a065

[4] Yamamoto, J., Tan, A., Shiratsuchi, R., Hayase, S., Chenthamarakshan, C.R. and Rajeshwar, K. (2003) A 4% Efficient Dye-Sensitized Solar Cell Fabricated from Cathodically Electrosynthesized Composite Titania Films. *Advanced Materials*, **15**, 1823-1825. http://dx.doi.org/10.1002/adma.200305239

[5] Radecka, M. and Rekas, M. (2002) Effect of High-Temperature Treatment on n-p Transition in Titania. *Journal of the American Ceramic Society*, **85**, 346-354. http://dx.doi.org/10.1111/j.1151-2916.2002.tb00095.x

[6] Wijnhoven, J.E. and Vos, W.L. (1998) Preparation of Photonic Crystals Made of Air Spheres in Titania. *Science*, **281**, 802-804. http://dx.doi.org/10.1126/science.281.5378.802

[7] Wu, J.-M., Hayakawa, S., Tsuru, K. and Osaka, A. (2002) *In Vitro* Bioactivity of Anatase Film Obtained by Direct Deposition from Aqueous Titanium Tetrafluoride Solutions. *Thin Solid Films*, **414**, 275-280. http://dx.doi.org/10.1016/S0040-6090(02)00498-4

[8] Tang, C., Fan, S., Lamy de la Chapelle, M., Dang, H. and Li, P. (2000) Synthesis of Gallium Phosphide Nanorods. *Advanced Materials*, **12**, 1346-1348. http://dx.doi.org/10.1002/1521-4095(200009)12:18<1346::AID-ADMA1346>3.0.CO;2-8

[9] Zhang, D.F., Sun, L.D., Yin, J.L. and Yan, C.H. (2003) Low-Temperature Fabrication of Highly Crystalline SnO_2 Nanorods. *Advanced Materials*, **15**, 1022-1025. http://dx.doi.org/10.1002/adma.200304899

[10] Sugimoto, T., Zhou, X. and Muramatsu, A. (2003) Synthesis of Uniform Anatase TiO_2 Nanoparticles by Gel–Sol Method: 4. Shape Control. *Journal of Colloid and Interface Science*, **259**, 53-61. http://dx.doi.org/10.1016/S0021-9797(03)00035-3

[11] Yang, K., Zhu, J., Zhu, J., Huang, S., Zhu, X. and Ma, G. (2003) Sonochemical Synthesis and Microstructure Investigation of Rod-Like Nanocrystalline Rutile Titania. *Materials Letters*, **57**, 4639-4642. http://dx.doi.org/10.1016/S0167-577X(03)00376-8

[12] Pradhan, S.K., Reucroft, P.J., Yang, F. and Dozier, A. (2003) Growth of TiO_2 Nanorods by Metalorganic Chemical Vapor Deposition. *Journal of Crystal Growth*, **256**, 83-88. http://dx.doi.org/10.1016/S0022-0248(03)01339-3

[13] Ayers, M. and Hunt, A. (1998) Titanium Oxide Aerogels Prepared from Titanium Metal and Hydrogen Peroxide. *Materials Letters*, **34**, 290-293. http://dx.doi.org/10.1016/S0167-577X(97)00181-X

[14] Song, K.C. and Pratsinis, S.E. (2000) The Effect of Alcohol Solvents on the Porosity and Phase Composition of Titania. *Journal of Colloid and Interface Science*, **231**, 289-298. http://dx.doi.org/10.1006/jcis.2000.7147

[15] Hu, Y., Tsai, H.-L. and Huang, C.-L. (2003) Effect of Brookite Phase on the Anatase-Rutile Transition in Titania Nanoparticles. *Journal of the European Ceramic Society*, **23**, 691-696. http://dx.doi.org/10.1016/S0955-2219(02)00194-2

[16] Ovenstone, J. and Chan, K.C. (2001) Effect of Halide Contaminant Ions in the Hydrothermal Treatment of Amorphous Titania on the Phase Change from Anatase to Rutile during Calcination. *European Journal of Inorganic Chemistry*, **5**, 1339-1342. http://dx.doi.org/10.1002/1099-0682(200105)2001:5<1339::AID-EJIC1339>3.0.CO;2-H

[17] Shimizu, K., Imai, H., Hirashima, H. and Tsukuma, K. (1999) Low-Temperature Synthesis of Anatase Thin Films on Glass and Organic Substrates by Direct Deposition from Aqueous Solutions. *Thin Solid Films*, **351**, 220-224. http://dx.doi.org/10.1016/S0040-6090(99)00084-X

[18] Yamabi, S. and Imai, H. (2002) Growth Conditions for Wurtzite Zinc Oxide Films in Aqueous Solutions. *Journal of Materials Chemistry*, **12**, 3773-3778. http://dx.doi.org/10.1039/b205384e

[19] Kolen'ko, Y.V. and Burukhin, A.A., Churagulov, B.R. and Oleynikov, N.N. (2003) Synthesis of Nanocrystalline TiO_2 Powders from Aqueous $TiOSO_4$ Solutions under Hydrothermal Conditions. *Materials Letters*, **57**, 1124-1129. http://dx.doi.org/10.1016/S0167-577X(02)00943-6

[20] Tengvall, P., Elwing, H. and Lundström, I. (1989) Titanium Gel Made from Metallic Titanium and Hydrogen Peroxide.

Journal of Colloid and Interface Science, **130**, 405-413. http://dx.doi.org/10.1016/0021-9797(89)90117-3

[21] Wang, X.X., Hayakawa, S., Tsuru, K. and Osaka, A. (2000) Improvement of Bioactivity of H_2O_2/$TaCl_5$-Treated Titanium after Subsequent Heat Treatments. *Journal of Biomedical Materials Research*, **52**, 171-176. http://dx.doi.org/10.1002/1097-4636(200010)52:1<171::AID-JBM22>3.0.CO;2-O

[22] Wu, J.-M., Zhang, T.-W., Zeng, Y.-W., Hayakawa, S., Tsuru, K. and Osaka, A. (2005) Large-Scale Preparation of Ordered Titania Nanorods with Enhanced Photocatalytic Activity. *Langmuir*, **21**, 6995-7002. http://dx.doi.org/10.1021/la0500272

[23] Porkodi, K. and Arokiamary, S. (2007) Synthesis and Spectroscopic Characterization of Nanostructured Anatase Titania: A Photocatalyst. *Materials Characterization*, **58**, 495-503. http://dx.doi.org/10.1016/j.matchar.2006.04.019

[24] Ba-Abbad, M.M., Kadhum, A., Al-Amiery, A.A., Mohamad, A. and Takriff, M.S. (2012) Toxicity Evaluation for Low Concentration of Chlorophenols under Solar Radiation Using Zinc Oxide (ZnO) Nanoparticles. *International Journal of Physical Sciences*, **7**, 48-52.

[25] Dolat, D., Quici, N., Kusiak-Nejman, E., Morawski, A. and Li Puma, G. (2012) One-Step, Hydrothermal Synthesis of Nitrogen, Carbon Co-Doped Titanium Dioxide (N, CTiO_2) Photocatalysts. Effect of Alcohol Degree and Chain Length as Carbon Dopant Precursors on Photocatalytic Activity and Catalyst Deactivation. *Applied Catalysis B*: *Environmental*, **115**, 81-89. http://dx.doi.org/10.1016/j.apcatb.2011.12.007